Applied Chemical Engineering (2024) Volume 7 Issue 4 ISSN: 2578-2010 (O)
doi: 10.59429/ace.v7i4.5584

ORIGINAL RESEARCH ARTICLE

Simulation of dielectric barrier discharge in argon-helium mixture for investigate the roles of plasma pressure and plasma temperature

Ismail Benchebiba[1, *], Mohamed Mostefaoui[1], Ahmed Nour El Islam Ayad[2], Abdelatif Gadoum[2]

[1] *LGEER Laboratory Faculty of Technology, Hassiba Benbouali University of Chlef, 02000, Algeria*

[2] *Electrical Engineering Department Faculty of Applied Sciences, Kasdi Merbah University of Ouargla, 30000, Algeria*

***Corresponding author:** Ismail Benchebiba, i.benchebiba@univ-chlef.dz

ABSTRACT

A one-dimensional fluid model is developed to analyze the effects of temperature and pressure on the characteristics of radiofrequency dielectric barrier discharge plasma. The model is run for an argon-helium mixture, in order to plot the maximum peak values of electron temperature, electric field strength and various species densities including electrons, atoms, ions and excited species as a function of plasma temperature in the range 300-550K, and as a function of plasma pressure in the range 0.2-1atm. The results show that an increase in the plasma temperature leads to an increase in electron temperature and electron density, and a decrease in electric field strength and non-electron species densities. In addition, an increase the plasma pressure leads to a decrease in electron temperature, an increase in electric field strength, and an increase in all species densities.

Keywords: argon; discharge; helium; plasma; pressure

ARTICLE INFO

Received: 8 December 2024
Accepted: 28 December 2024
Available online: 30 December 2024

1. Introduction

During the last decade, there has been a growing interest in modeling and simulation of various plasma processes. Plasma topics have included gas conversion, material modification, analytical chemistry, and other applications[1-4]. In the art of plasma there are several techniques, the most common being dielectric barrier discharge, corona discharge, inductively coupled and capacitively coupled plasma discharges[5-8]. Dielectric barrier discharge (DBD) is of great importance in engineering, science and technology due to its efficiency in cold and non-equilibrium plasma generation[9].Modeling and simulation as well as experimental studies of discharge plasma have been performed for a variety of working gases, including methane, argon, oxygen, nitrogen, air, helium, and air[10].

For example, Khadir N et al[11], studied a dielectric barrier discharge at atmospheric pressure for methane conversion and hydrogen production, and investigated some discharge parameters on the methane DBD characteristic, they found that increasing the gas pressure from 380 to 1520 Torr decreases the conversion and electron density, and increasing the gas temperature from 250 to 400 K has almost no effect on the conversion and slightly increases in the electron density. Benmoussa A et al[12], optimize the gas temperature along the axial distance from the cathode in methane DBD, and suggests that the discharge behavior and hydrogen production can be improved by various methods such as, increasing the applied voltage, gas pressure,

and dielectric capacitance, in a one-dimensional DBD model. Zhang Z et al[13], perform a fluid simulation of a pure argon dielectric barrier discharge by increasing the temperature from 300 to 600 K. They found a decrease in the ionization rate peak, the electron and ion densities, and an increase in the electron temperature peak with increasing gas temperature. Baeva M et al[14], reported that due to the dissociation of oxygen molecules, the energy lost by electrons in argon-oxygen mixture is important then in pure argon, which decreases the electron density and temperature in a modeling study of microwave generated plasma.

In this paper, a one-dimensional fluid model of dielectric barrier discharge is presented to study the effect of plasma pressure and plasma temperature on the properties of argon-helium mixture plasma. The characteristics studied are electron temperature, electric field strength, and various species densities, including electrons, argon atoms, argon ions, excited argon species, helium atoms, helium ions, and excited helium species. Six simulations are performed for six temperature values of 300, 350, 400, 450, 500, and 550 K, and nine simulations are performed for nine pressure values of 0.2, 0.3, 0.4, 0.5, 0.6, 0.7, 0.8, 0.9, and 1 atm. There are many studies of pure argon plasmas, but few of argon-helium mixtures. The contribution of this work is to enrich the scarce studies of argon-helium mixture plasmas. In each simulation run, the properties of the argon-helium mixture reach maximum values. These maxima are evaluated in terms of temperature in the range of 300-550 K and pressure in the range of 0.2-1 atm.

2. Materials and methods

2.1. Model presentation

Figure 1 (a) shows the two-dimensional configuration of the DBD reactor, and the corresponding one-dimensional model is shown in **Figure 1 (b)**. A high voltage is applied to the powered electrode, and the other electrode is grounded. The plasma gap is sandwiched by two dielectrics, the dielectric associated with the powered electrode is called the powered dielectric, and the dielectric associated with the grounded electrode is called the grounded dielectric. The applied voltage is sinusoidal with a peak of 1kV and a frequency of 13.56 MHz frequency. The relative permittivity of the two dielectrics is 10. The thickness of the dielectrics and the plasma gap is sited 0.1 mm. In the plasma gap, the densities of electrons, argon ions and helium ions are initiated at 2×10^{-13} m^{-3}, 1×10^{-13} m^{-3}, and 1×10^{-13} m^{-3} respectively.

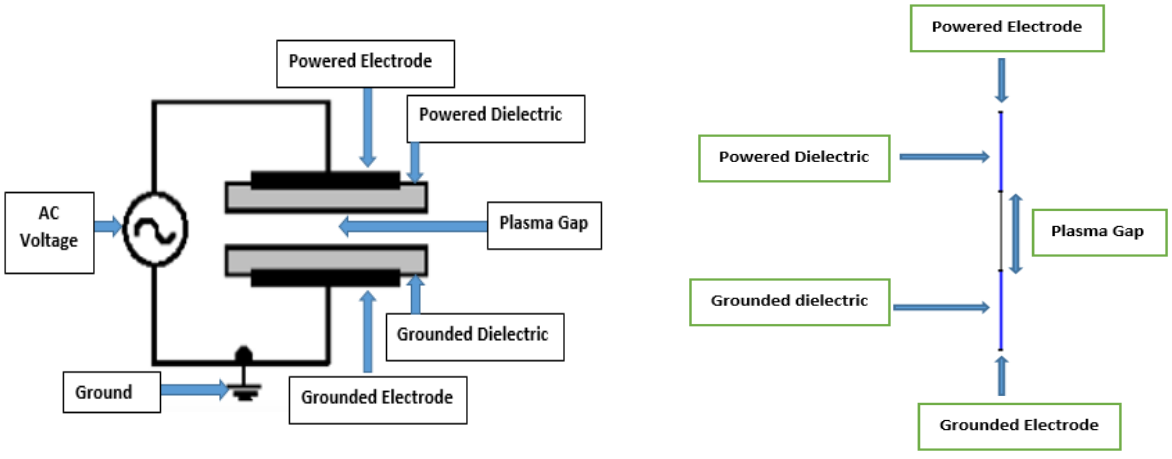

(a) **(b)**

Figure 1. DBD model geometry: **(a)** Two-dimensional configuration of DBD ; **(b)** Corresponding one dimensional model.

2.2. Chemical reactions

The chemical reactions considered in the simulation are listed in **Table 1**. Where e is the electron, He is the helium atom, He* is the excited helium, He+ is the helium ion, Ar is the argon atom, Ar* is the excited

argon, and Ar+ is the argon ion. The symbol f(ε) refers to the collision cross section as a function of the electron energy ε for the electron impact reactions.

Table 1. List of chemical reactions included in the model.

No	Reaction	Rate constant (cm^3/s)	Reference
R1	$e + He \rightarrow e + He$	f(ε)	[15,16]
R2	$e + He \rightarrow e + He^*$	f(ε)	[15,16]
R3	$e + He \rightarrow 2e + He^+$	f(ε)	[15,16]
R4	$e + Ar \rightarrow e + Ar$	f(ε)	[17]
R5	$e + Ar \rightarrow e + Ar^*$	f(ε)	[17]
R6	$e + Ar^* \rightarrow e + Ar$	f(ε)	[17]
R7	$e + Ar \rightarrow 2e + Ar^+$	f(ε)	[17]
R8	$e + Ar^* \rightarrow 2e + Ar^+$	f(ε)	[17]
R9	$Ar^* + Ar^* \rightarrow e + Ar + Ar^+$	6.2×10^{-10}	[18,19]
R10	$Ar^* + Ar \rightarrow Ar + Ar$	3×10^{-15}	[18,19]

2.3. Model equations and boundary conditions

At the powered electrode, the applied voltage boundary condition formula is as follows:

$$V(t) = -V_{max}Sin(2\pi ft) \quad (1)$$

Where V_{max} is the peak applied voltage, f is the voltage frequency and t is the time.

At the powered dielectric surface and the grounded dielectric surface, the flux boundary conditions are for ions J_i and electrons J_e:

$$J_i = \mu_i n_i E \quad (2)$$

$$J_e = -\gamma J_i - k_s n_e \quad (3)$$

Where γ is the secondary electron emission coefficient, k_s is the electron recombination coefficient, E is the electric field, μ_i is the ion mobility, n_i and n_e are the ion and electron densities, respectively.

At the grounded electrode, the electric potential must be zero by the following boundary condition:

$$V = 0 \quad (4)$$

The surface charge accumulation occurs at the interface between the dielectric layer and the plasma gap. This phenomenon leads to a boundary condition on the dielectric barriers, which can be expressed as follows:

$$\varepsilon_r\varepsilon_0 E_{Dielectric} - \varepsilon_0 E_{Plasma} = \rho_s \quad (5)$$

Where $E_{Dielectric}$ and E_{Plasma} are the electric fields at the dielectric interfaces, and ε_0 and ε_r are the vacuum permittivity and dielectric relative permittivity, respectively, and ρ_s is the surface charge density.

The continuity equation for electrons, ions and excited species is presented by:

$$\partial n/\partial t + \nabla \Gamma = S \quad (6)$$

Where n, Γ and S are the species density, flux and source term, respectively.

The drift-diffusion equation for electrons and ions and is approximated by:

$$\Gamma = -n\mu E - \nabla(nD) \quad (7)$$

Where D is the species mobility.

The electric field is related to the electric potential using Poisson's Equation as follows:

$$E = -\nabla V \quad (8)$$

3. Results and discussion

3.1. Calculated maximum values of Ar/He DBD characteristics

The calculated initial maximum values of the argon-helium plasma properties for the two scenarios are tabulated in **Table 2**. The changes in these values as a function of temperature and pressure are discussed later.

Table 2. Calculated initial maximum values of Ar/He DBD characteristics.

Ar/He DBD characteristics	T=300 K at 1 atm Pressure	P= 0.2 atm at 400 K Temperature
Electron temperature (eV)	14.2	40.9
Electric field strength (kV/mm)	39.3	34.3
Electron density (m^{-3})	1.57×10^{20}	4.45×10^{19}
Ar density (m^{-3})	2.45×10^{25}	3.67×10^{24}
Ar^* density (m^{-3})	1.37×10^{21}	5.9×10^{20}
Ar^+ density (m^{-3})	2.26×10^{20}	5.09×10^{19}
He density (m^{-3})	4.87×10^{17}	7.24×10^{16}
He^* density (m^{-3})	2.45×10^{17}	5.9×10^{20}
He^+ density (m^{-3})	1.15×10^{13}	1.03×10^{13}

3.1.1. Results of electron temperature

Figure 2 (a) shows the variation of electron temperature as a function of plasma temperature in the range of 300-550K at atmospheric pressure. The electron temperature increases as the plasma temperature increases, which is in consistent with theoretical expectations. The electron temperature increases from 14.2 eV at 300 K to 20.1 eV at 550 K. **Figure 2 (b)** shows the electron temperature variation as a function of plasma pressure in the range of 0.2-1atm at 400 K plasma temperature. The electron temperature decreases with increasing plasma pressure. It drops from 40.9 eV at 0.2 atm to 17.3 eV at 1 atm.

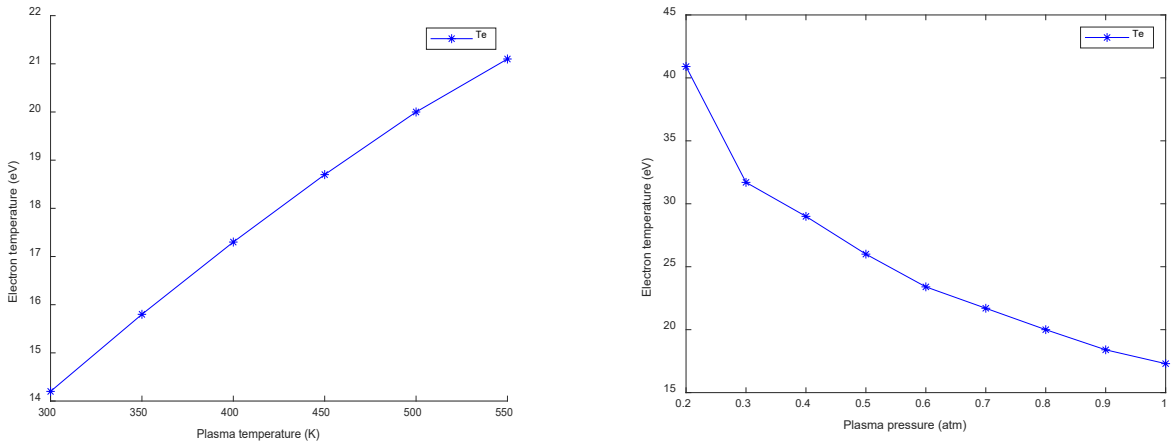

(a) (b)

Figure 2. Results of electron temperature: **(a)** As a function of plasma temperature in range 300-550K at atmospheric pressure; **(b)** As a function of plasma pressure in range 0.2-1atm at 400 K temperature.

3.1.2. Results of electric field strength

Figure 3 (a) shows the variation of the electric field strength as a function of plasma temperature. The electric field strength value increases from 39.3 kV/mm to 33.8 kV/mm as the plasma temperature increases

from 300 to 550 K. **Figure 3 (b)** shows the variation of the electric field strength as a function of plasma pressure. The electric field strength increases from 24.3 kV/mm at 0.2 atm to 36.7 kV/mm at 1atm.

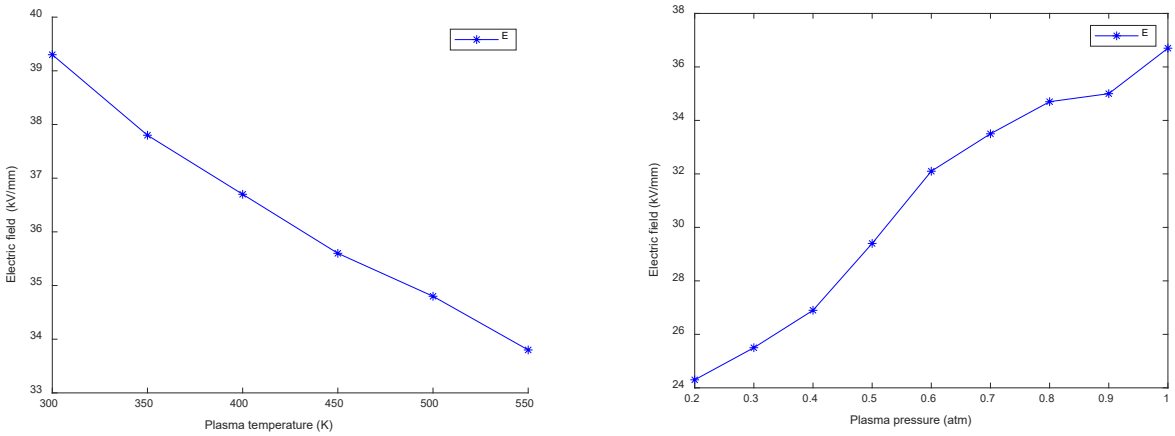

(a) (b)

Figure 3. Results of electric field strength: **(a)** As a function of plasma temperature in range 300-550 K at atmospheric pressure; **(b)** As a function of plasma pressure in range 0.2-1atm at 400 K temperature.

3.1.3. Results of electron density

Figure 4 (a) shows the variation of the electron density value variation as a function of plasma temperature. The electron density value decreases from 1.57×10^{20} to 1.55×10^{20} m^{-3} between 300 and 350 K, increases from 1.55×10^{20} to 1.79×10^{20} m^{-3} between 350 and 500 K, and remains stable at 1.79×10^{20} m^{-3} between 500 and 550 K. **Figure 4 (b)** shows the electron density value variation as a function of plasma pressure. The electron density decreased slowly from 4.45×10^{19} to 4.38×10^{19} m^{-3} between 0.2 and 0.3 atm , increased rapidly from 4.38×10^{19} to 1.81×10^{20} m^{-3} between 0.3 and 0.8 atm , decreased from 1.81×10^{20} to 1.67×10^{20} m^{-3} between 0.8 and 1atm. The change in electron density is not expected to be monotonic with temperature or pressure. Due to its unique properties compared to non-electron species, the electron has a negative electric charge and a very small mass, which makes predicting changes in its density counterintuitive. However, the electron density can be assumed to be directly proportional to temperature and pressure in certain ranges, with the exception of others. The electron density variations depend mainly on the working gas and pressure range in which the electron density is evaluated.

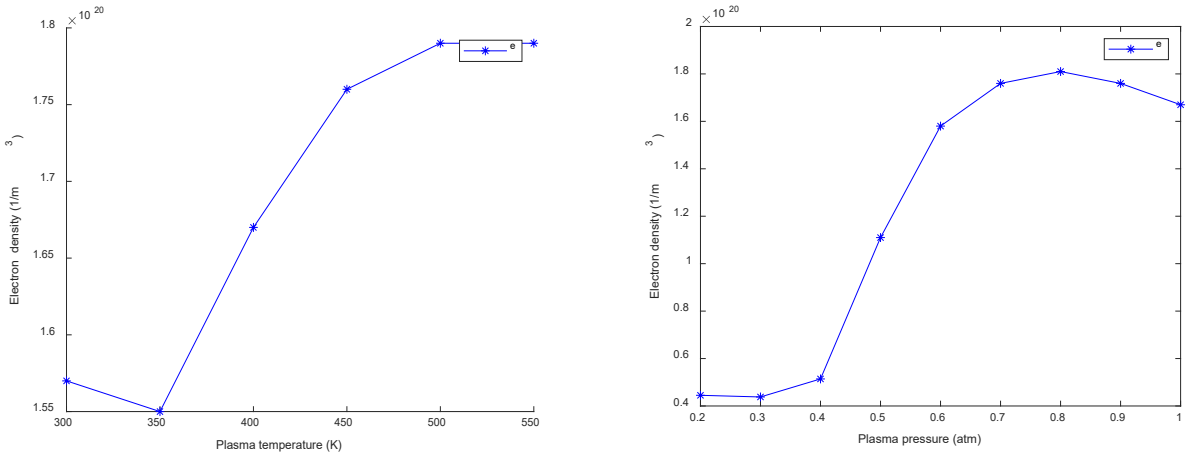

(a) (b)

Figure 4. Results of electron density: **(a)** As a function of plasma temperature in range 300-550 K at atmospheric pressure; **(b)** As a function of plasma pressure in range 0.2-1atm at 400 K temperature.

3.1.4. Results of argon atom density

Figure 5 (a) shows the variation of the Ar density value as a function of plasma temperature. The Ar density value decreases from 2.45×10^{25} to 1.33×10^{25} m^{-3} as the plasma temperature increases from 300 to 550 K. **Figure 5 (b)** shows the variation of Ar density as a function of plasma pressure. The Ar density is increased from 3.67×10^{24} m^{-3} at 0.2 atm to 1.83×10^{25} m^{-3} at 1atm. There is a monotonic decrease in the density of Ar as a function of temperature and a monotonic increase in the density of Ar as a function of pressure.

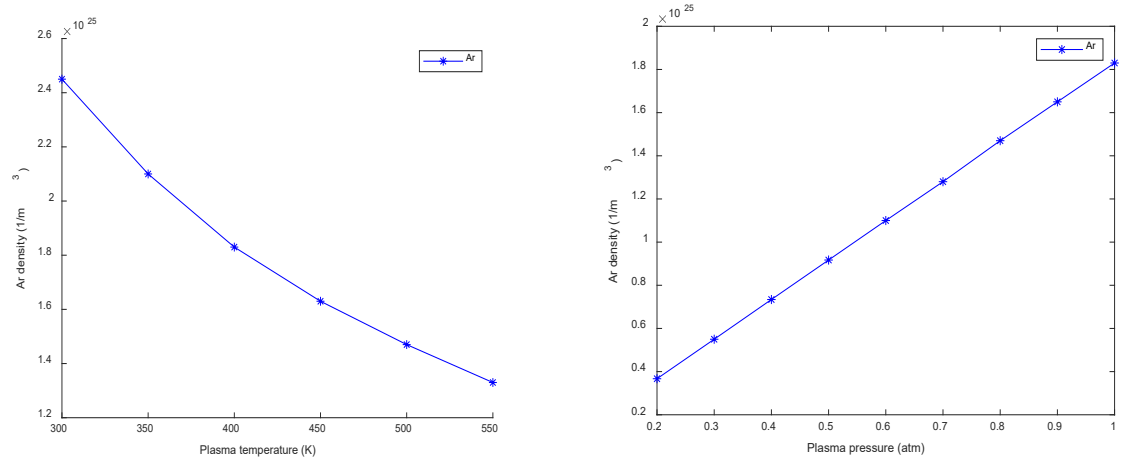

(a) (b)

Figure 5. Results of Ar density: **(a)** As a function of plasma temperature in range 300-550 K at atmospheric pressure; **(b)** As a function of plasma pressure in range 0.2-1atm at 400 K temperature.

3.1.5. Results of excited argon density

Figure 6 (a) shows the variation of Ar^* density value as a function of plasma temperature. The value of Ar^* density decreases from 1.37×10^{21} to 9.15×10^{20} m^{-3} as the plasma temperature increases from 300 to 550 K. **Figure 6 (b)** shows the variation of Ar^* density as a function of plasma pressure. The Ar^* density increases as the plasma pressure increases, from 5.9×10^{20} m^{-3} at 0.2 atm to reach the value of 1.15×10^{21} m^{-3} at 1 atm. The excited specie Ar^* is mainly produced by the reaction R5 between e and Ar , losses through the reactions R6, R8-R10 to reform Ar and Ar^+, which relate its density variation to the Ar density variation, it is decreased when the Ar density decreased and vice versa.

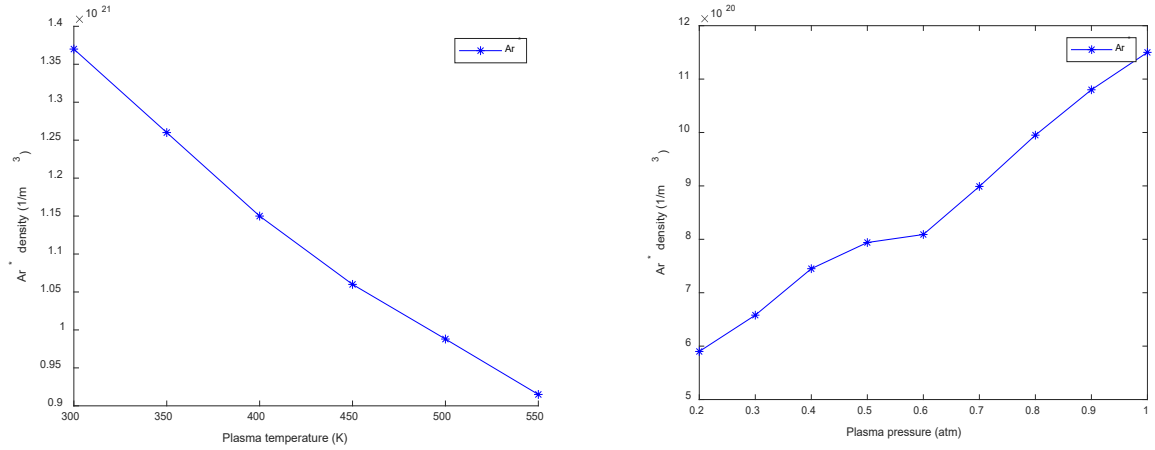

(a) (b)

Figure 6. Results of Ar^* density : **(a)** As a function of plasma temperature in range 300-550 K at atmospheric pressure ; **(b)** As a function of plasma pressure in range 0.2-1atm at 400 K temperature.

3.1.6. Results of argon ion density

Figure 7 (a) shows the variation of the Ar^+ density value as a function of plasma temperature. The value of Ar^+ density decreases from 2.26×10^{20} to 1.76×10^{20} m^{-3} between 300 and 450 K, increases from 1.76×10^{20} to 1.79×10^{20} m^{-3} between 450 and 550 K, and remains stable at 1.79×10^{20} m^{-3} between 500 and 550 K. **Figure 7 (b)** shows the variation of Ar^+ density as a function of plasma pressure. The Ar^+ density increases from 5.09×10^{19} to 1.81×10^{20} m^{-3} between 0.2 and 0.8 atm, decreases from 1.81×10^{20} to 1.76×10^{20} m^{-3} between 0.8 and 0.9 atm, and increases from 1.76×10^{20} to 1.87×10^{20} m^{-3} between 0.9 and 1 atm. As an ion, the change in its number density is related to the change in the electron density and/or the density of the species formed from it. The ion Ar^+ is formed by the reaction R7 between e and Ar, the reaction R8 between e and Ar^*, and the reaction R9 between Ar^* and Ar^*. In the temperature range of 300-450K, the Ar^+ density increased as the densities of Ar and Ar^* well, but then it increased in the temperature range of 450-500 K, stable in the temperature range of 500-550 K as the electrode density well. In the 0.2-0.8 atm pressure range, the Ar^+ density increased as the densities of Ar and Ar^* increased , but it decreased between 0.8 and 0.9 atm as the electron density decreased , then increased between 0.9 and 0.1 atm as the densities of Ar and Ar^* increased. This contrast proves that there are certain temperature and pressure ranges where the change in ion density follows the same path as the change in electron density rather than the change in the atoms or excited species from which the ion is formed.

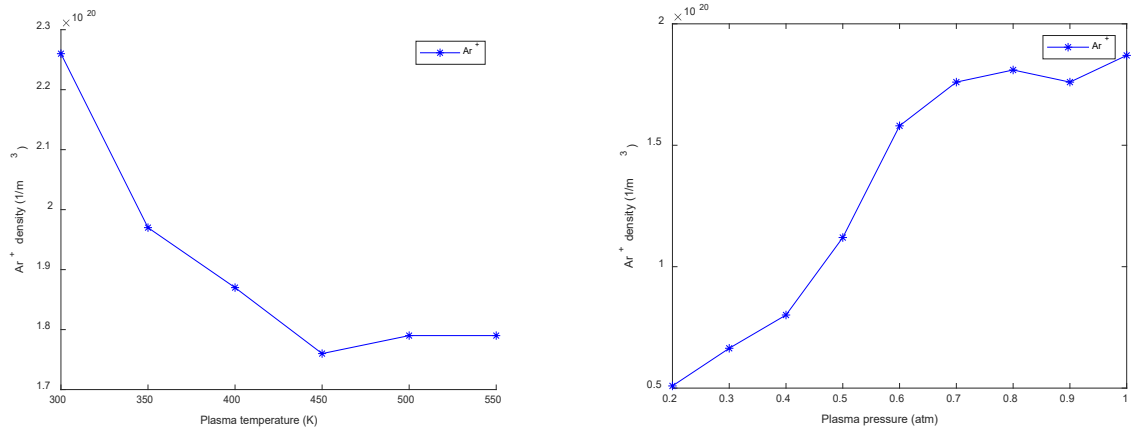

(a) **(b)**

Figure 7. Results of Ar^+ density: **(a)** As a function of plasma temperature in range 300-550 K at atmospheric pressure; **(b)** As a function of plasma pressure in range 0.2-1atm at 400 K temperature.

3.1.7. Results of helium atom density

Figure 8 (a) shows the variation of the He density value as a function of plasma temperature. The value of He density decreases from 4.87×10^{17} to 2.65×10^{17} m^{-3} as the plasma temperature increases from 300 to 550 K. The He density increases with the increase of plasma pressure, from 7.24×10^{16} m^{-3} at 0.2 atm to 3.65×10^{17} m^{-3} at 1 atm as shown in **Figure 8 (b)**. There is a monotonic decrease in the He density as a function of temperature and a monotonic increase in the He density as a function of pressure. As in the case of the Ar density, the densities of neutral species changes vary directly with the temperature and inversely with the pressure.

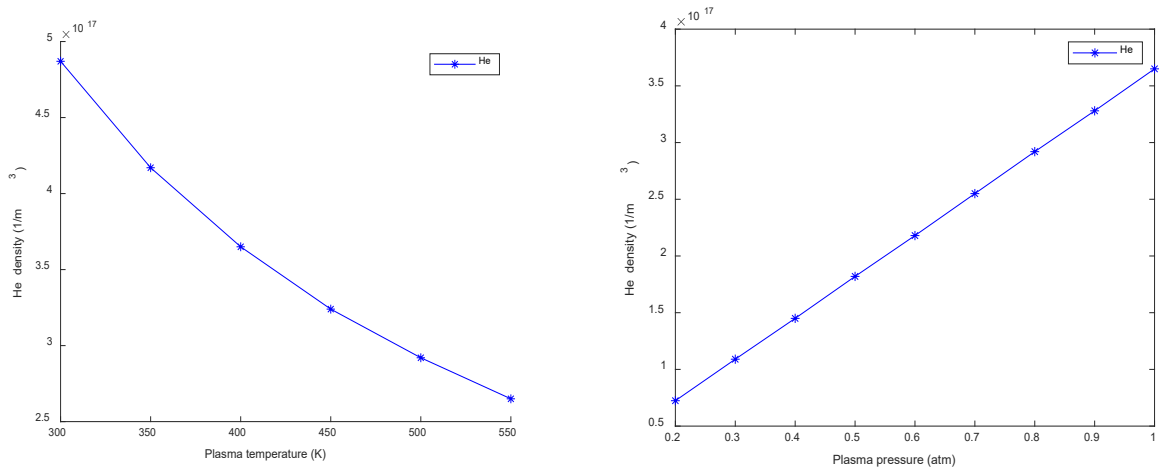

(a) (b)

Figure 8. Results of He density: **(a)** as a function of plasma temperature in range 300-550 K at atmospheric pressure; **(b)** as a function of plasma pressure in range 0.2-1atm at 400 K temperature.

3.1.8. Results of excited helium density

Figure 9 (a) shows the variation of the He^* density value as a function of plasma temperature. The value of He^* density decreases from 2.45×10^{17} to 1.33×10^{17} m^{-3} as the plasma temperature increases from 300 to 550 K. **Figure 9 (b)** shows the variation of He^* density as a function of plasma pressure. The He^* density increases with increasing plasma pressure, from 3.67×10^{16} m^{-3} at 0.2 atm to reach the value of 1.83×10^{17} m^{-3} at 1atm. The excited specie He^* is produced by the reaction R2 between e and He, which directly relate the change of its density directly to the change of the He density. It increases when the He density increases and vice versa.

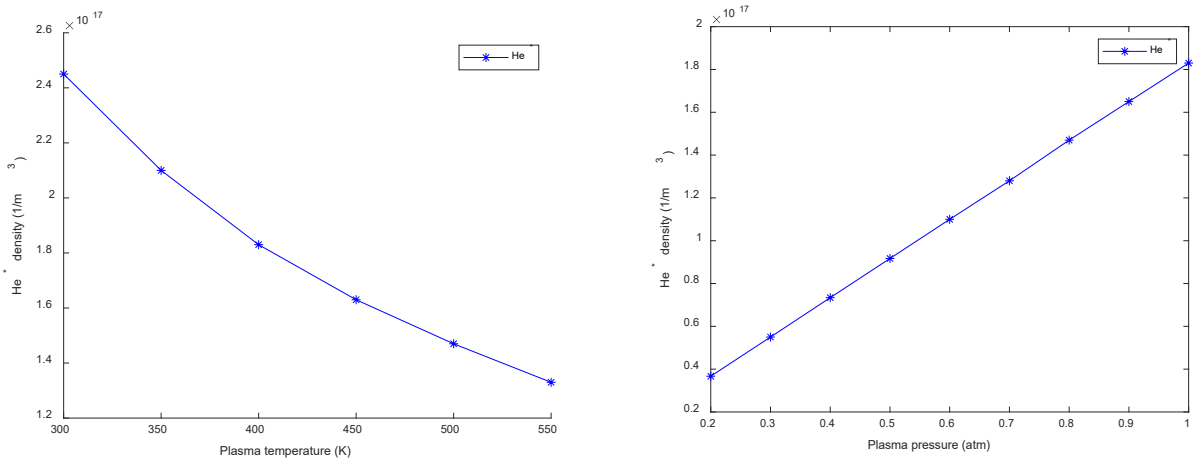

(a) **(b)**

Figure 9. Results of He^* density : **(a)** as a function of plasma temperature in range 300-550 K at atmospheric pressure ; **(b)** as a function of plasma pressure in range 0.2-1atm at 400 K temperature.

3.1.9. Results of helium ion density

Figure 10 (a) shows the variation of the He^+ density value as a function of plasma temperature. The value of He^+ density decreases from 1.15×10^{13} to 1.09×10^{13} m^{-3} as the plasma temperature increases from 300 to 550 K. **Figure 10 (b)** shows the variation of He^+ density as a function of plasma pressure. The He^+ density increases between 0.2 and 0.4 atm from 1.03×10^{13} to 1.08×10^{13} m^{-3}, decreases between 0.4 and 0.5 atm from 1.08×10^{13} to 1.06×10^{13} m^{-3}, increases between 0.5 and 1 atm, from 1.06×10^{13} to 1.12×10^{13} m^{-3}. The ion He^+ is produced by the reaction R3 between e and He. The He^+ density decreases as a function of temperature, as

do the densities of He and He^*. The He^+ density is increased as a function of pressure, as the densities of He and He^* well, expect for the pressure range 0.4-0.5 atm in which the He^+ density is decreased.

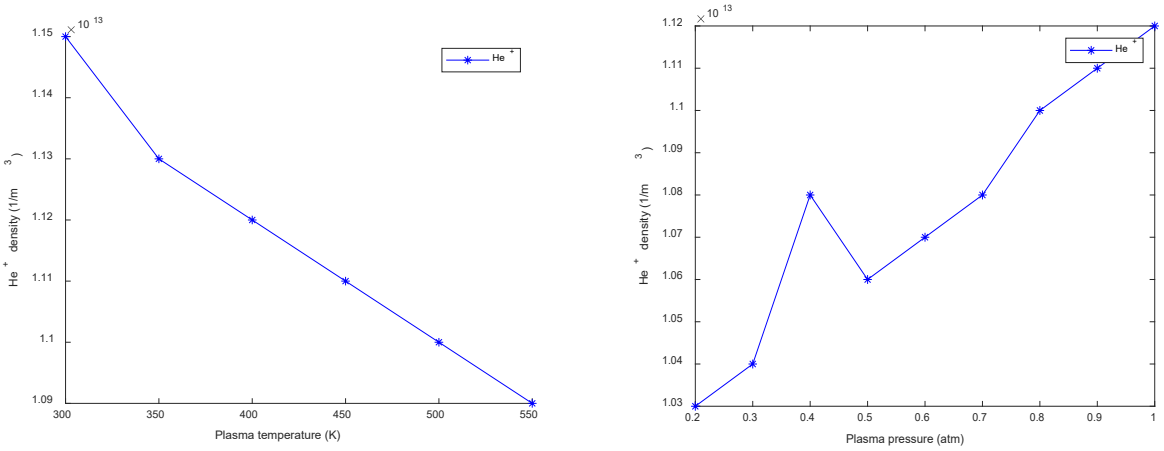

(a) (b)

Figure 10. Results of He^+ density: **(a)** as a function of plasma temperature in range 300-550 K at atmospheric pressure; **(b)** as a function of plasma pressure in range 0.2-1atm at 400 K temperature.

4. Conclusion

In this paper, a one-dimensional fluid model of dielectric barrier discharge operating in a mixture of argon and helium is established. The aim was to investigate the effects of temperature and pressure, on the variations of electron temperature, electric field strength and different species densities. The obtained results show that, with increasing the temperature from 300 to 550 K, the electron temperature increases, the electric field strength decreases, the electron density decreases between 300 and 350 K, then it increases between 350 and 500 K, stable between 500 and 500 K, the Ar^+ density decreases between 300 and 450 K, increases between 450 and 500 K, stable between 500 and 550 K, and the densities of Ar , Ar^* , He , He^* , and He^+ decrease. With the increase of pressure from 0.2 to 1 atm, the electron temperature decreases, the electric field strength increases, the electron density decreases slowly between 0.2 and 0.3 atm , increases rapidly between 0.3 and 0.8 atm, decreases between 0.8 and 1atm, the Ar^+ density increases between 0.2 and 0.8 atm, decreases between 0.8 and 0.9 atm ,increases between 0.9 and 1 atm, the He^+ density increases between 0.2 and 0.4 atm, decreases between 0.4 and 0.5 atm , increases between 0.5 and 1 atm, the densities of Ar, Ar^*, He, and He^* increase.

Conflict of interest

The authors declare no conflict of interest.

References

1. Hegemann D, Barkhordari A, Mirzaei SI, et al. Experimental Study of a Rotating Electrode Plasma Reactor for Hydrogen Production from Liquid Petroleum Gas Conversion. Applied Sciences 2022; 12(8): 4045. https://doi.org/10.3390/app12084045

2. Sun X, Bao J, Li K, et al. Advance in using plasma technology for modification of carbon-based materials and their applications in environmental, material, and energy fields. Advanced Functional Materials 2021; 31(7): 2006287. https://doi.org/10.1002/adfm.202006287

3. Papadimas V, Doudesis C, Svarnas P, et al. SDBD flexible plasma actuator with Ag-Ink electrodes: experimental assessment. Applied Sciences 2021; 11(24): 11930. https://doi.org/10.3390/app112411930

4. Domonkos M, Tichá P, Trejbal J, et al. Applications of Cold Atmospheric Pressure Plasma Technology in Medicine, Agriculture and Food Industry 2021 ;11(11) ; 4809 https://doi.org/10.3390/app11114809

5. Wilde N D, Xu H, Gomez-Vega N. A model of surface dielectric barrier discharge power. Applied Physics Letters 2021; 118(15): 154102. https://doi.org/10.1063/5.004339

6. El-Tayeb A, El-Dein AZ, Elnaggar AY, et al. Influence of temperature in degradation of organic pollution using corona discharge plasma. Sustainability 2021; 13(23): 12971. https://doi.org/10.3390/su132312971

7. Yoon MY, Yeom HJ, Kim JH, et al. Discharge physics and atomic layer etching in Ar/C4H6 inductively coupled plasma with a radio frequency bias. Physics of Plasmas 2021; 28(6): 063504. https://doi.org/10.1063/5.0047811

8. Wen DQ, Krek J, Gudmundsson JT, et al. On the importance of excited state species in low pressure capacitively coupled plasma argon discharges. Plasma Sources Sciences and Technology 2023; 32(6): 064001. https://doi.org/10.1088/1361-6595/acd6b4

9. Arserim EH, Salvi D, Fridman G, et al. Microbial Inactivation by Non-equilibrium Short-Pulsed Atmospheric Pressure Dielectric Barrier Dischrage (Cold Plasma): Numerical and Experimental Studies. Food Eng Rev 2021; 13 : 136-147 https://doi.org/10.1007/s12393-020-09256-7

10. Svarnas P, Papadopoulos PK, Vafeas P, et al. Influence of atmospheric pressure guided streamers (plasma bullets) on the working gas patters in air. IEEE Transactions on Plasma Science 2014 ; 42(10) : 2430-2431 https://doi.org/10.1109/TPS.2014.2322098

11. Khadir N, Khodja K, Belasri A. Methane conversion using a dielectric barrier discharge reactor at atmospheric pressure for hydrogen production. Plasma Science and Technology 2017; 19(9): 095502. https://doi.org/10.1088/2058-6272/aa6d6d

12. Benmoussa A, Belasri A, Larouci B. Gas Temperature Effect in Methane DBD Reactor for Hydrogen Production. Plasma Medicine 2022 ; 12(3) ; 41-58 https://doi.org/10.1615/PlasmaMed.2023047179

13. Zhang Z, Zhong KX, Liu Y, et al. Fluid simulation of atmospheric argon RF dielectric barrier discharges: Role of natural gas temperature. Physics of Plasmas 2024; 13(5): 053515. https://doi.org/10.1063/5.0202078

14. Baeva M, Stankov M, Trautvetter TJ. The effect of oxygen admixture on the properties of microwave generated plasma in Ar-O_2: A modelling study. Journal of Physics D: Applied Physics 2021; 54(35): 355205. https://doi.org/10.1088/1361-6463/ac08cc

15. Ran S, Wang J, Lei B, et al. Numerical simulation of coaxial-coplanar dielectric barrier discharge in atmospheric helium. AIP Advances. 2022; 12(5): 055209. https://doi.org/10.1063/5.0089080

16. Hagelaar GJM, Pitchford LC. Solving the Boltzmann equation to obtain electron transport coefficients and rate coefficients for fluid models. Plasma sources science and technology. 2005; 14(4): 722. https://doi.org/10.1088/0963-0252/14/4/011

17. Yanguas-Gil A, Cotrino J, Alves LL. An update of argon inelastic cross sections for plasma discharges. Journal of Physics D: Applied physics. 2005; 38(10): 1588. https://doi.org/10.1088/0022-3727/38/10/014

18. Baeva M, Hemel F, Baierl H, et al. Two-and three-dimensional simulation analysis of microwave excited plasma for deposition applications: operation with argon at atmospheric pressure. Journal of Physics D: Applied Physics. 2018; 51(38): 385202. https://doi.org/10.1088/1361-6463/aad537

19. Lymberpoulos DP, Economou DJ. Fluid simulation of glow discharge: Effect of metastable atoms in argon. Journal of Applied Physics 1993; 73(8): 3668-3679. https://doi.org/10.1063/1.352926